

HMOE: Hypernetwork-based Mixture of Experts for Domain Generalization

Jingang Qu¹ Thibault Faney² Ze Wang¹ Patrick Gallinari^{1,3}
Soleiman Yousef² Jean-Charles de Hemptinne²

Sorbonne Université, CNRS, ISIR, F-75005 Paris, France¹ IFPEN² Criteo AI Lab, Paris³

Abstract

Due to domain shift, machine learning systems typically fail to generalize well to domains different from those of training data, which is what domain generalization (DG) aims to address. Although various DG methods have been developed, most of them lack interpretability and require domain labels that are not available in many real-world scenarios. This paper presents a novel DG method, called HMOE: Hypernetwork-based Mixture of Experts (MoE), which does not rely on domain labels and is more interpretable. MoE proves effective in identifying heterogeneous patterns in data. For the DG problem, heterogeneity arises exactly from domain shift. HMOE uses hypernetworks taking vectors as input to generate experts' weights, which allows experts to share useful meta-knowledge and enables exploring experts' similarities in a low-dimensional vector space. We compare HMOE with other DG algorithms under a fair and unified benchmark-DomainBed. Our extensive experiments show that HMOE can divide mixed-domain data into distinct clusters that are surprisingly more consistent with human intuition than original domain labels. Compared to other DG methods, HMOE shows competitive performance and achieves SOTA results in some cases.

1. Introduction

Domain generalization (DG) aims to train models on known domains that can generalize well to unseen domains, which is of crucial importance for deploying models in safety-critical real-world applications. Over the past decade, a variety of DG algorithms have been proposed [26, 95, 85], focusing primarily on developing DG-specific data augmentation techniques and learning domain-invariant representations to build generalizable predictors. However, many high-performing DG algorithms rely on domain labels to explicitly reduce domain discrepancy, severely limiting their applicability in real-world scenarios where domain annotation may be prohibitively expensive. Additionally, current DG algorithms lack interpretability

and fail to provide insight into the causes of success or failure in generalizing to new domains. Therefore, the goal of this work is to develop a novel DG algorithm which does not require domain labels and is more interpretable.

We follow the nomenclature of [9], which refers to DG with domain labels as vanilla DG and the more challenging DG without domain labels as compound DG. Our work focuses on addressing compound DG through inferring latent domains from mixed-domain data and using them efficiently. [12, 5, 56] demonstrated that using domain-wise datasets can theoretically achieve lower generalization error bounds and better DG performance than using mixed data directly, indicating the importance of domain information. Furthermore, latent domain discovery helps us understand the workings of models and enhances interpretability. To make the problem tractable, we assume that latent domains are distinct and separable.

In this paper, we propose HMOE: Hypernetwork-based Mixture of Experts (**MoE**). MoE is a well-established learning paradigm that aggregates a number of experts by calculating the weighted sum of their predictions [34, 35], where the aggregation weights, also known as gate values, are determined by a routing mechanism and add up to 1. To discover latent domains, HMOE leverages MoE's *divide and conquer* property, that is, the routing mechanism can learn to softly partition the input space into subspaces in an unsupervised manner during training [89], with each assigned to an expert. We further expect that each subspace is associated with a latent domain, enabling latent domain discovery. During inference, we can compare the similarities between an unseen test domain and the inferred domains based on gate values, hence improving interpretability. [27, 94] have validated MoE in domain adaptation [86] and mentioned that MoE can leverage the specialty of individual domain and alleviate negative knowledge transfer [73] compared to using a single model to learn multiple different domains.

HMOE innovatively uses a neural network, called a hypernetwork [28], which takes vectors as input to generate the weights of experts of MoE. By mapping vectors into experts, hypernetworks enable the exploration of experts' similarities in a low-dimensional vector space, facilitating

latent domain discovery. Hypernetworks also serve as a link between experts, providing a platform for them to exchange information and promoting knowledge sharing.

MoE’s intrinsic soft partitioning is not always effective and sometimes fails to maintain a consistent division of the input space, especially when the distinction between latent domains is not significant. To address this issue, we propose a differentiable dense-to-sparse Top-1 routing algorithm, which forces gate values to become one-hot and converges to hard partitioning. This leads to sparse-gated MoE, which improves and stabilizes latent domain discovery. In addition, to better incorporate hypernetworks into MoE, we introduce an embedding space that contains a set of learnable embedding vectors corresponding one-to-one with experts. This embedding space is fed to hypernetworks to generate the weights of experts and is also part of the routing mechanism to compute gate values, thus enhancing the interaction between hypernetworks and the routing mechanism.

We summarize our contributions as follows: (1) We present a novel DG method, HMOE, within the framework of MoE. HMOE does not require domain labels, enables latent domain discovery, and offers excellent interpretability. (2) HMOE innovates the use of hypernetworks to generate expert weights and achieves sparse-gated MoE. (3) As far as we know, HMOE is the first work that can jointly learn and utilize latent domains in an end-to-end way. (4) We conduct comprehensive experiments to compare HMOE with other DG methods under a fair and unified evaluation framework – DomainBed [26]. HMOE achieves competitive performance and even state-of-the-art results in some cases.

2. Related Work

2.1. Domain Generalization (DG)

The goal of DG is to train a predictor on known domains that can generalize well to unseen domains.

Vanilla DG The first line of work is to design DG-specific data augmentation techniques to increase the diversity and quantity of training data to improve DG performance [88, 82, 68, 90, 49, 98, 63, 96]. Previous work learned domain-invariant representations through invariant risk minimization [2, 39, 1], kernel methods [56, 23, 20, 5], feature alignment [59, 76, 84, 74, 61, 45, 55, 24, 54], and domain-adversarial training [21, 22, 45, 47, 25]. Another approach is to disentangle latent features into class-specific and domain-specific representations [36, 62, 33, 57, 91]. General machine learning paradigms were also applied to vanilla DG, such as meta-learning [42, 3, 15, 44], self-supervised learning [7, 37], gradient manipulation [32, 70, 64], and distributionally robust optimization [65, 39].

Compound DG There are some DG algorithms that do not require domain labels by design [32, 54, 46, 57, 91, 9]. Besides improving DG performance, latent domain discov-

ery is also an important task for compound DG and contributes to better interpretability. [54, 9] can do this but have two main limitations: (1) Their methods proceed in two phases: first infer latent domains from mixed data and then deal with DG using the inferred domains, which is similar to vanilla DG. The problem is that the second phase depends on the first and cannot provide some feedback to correct possible errors in domain discovery. (2) Their methods assume that domain shift arises from stylistic differences to identify latent domains, which does not always hold.

On the contrary, HMOE is trained in an end-to-end manner and leverages MoE to discover latent domains without an explicit induced bias on the cause of domain shift.

2.2. Hypernetworks

A hypernetwork is a neural network that generates the weights of another target network. Hypernetworks were initially proposed by [28] and have since been applied to optimization problems [51, 58], meta-learning [93], continuous learning [83, 6], multi-task learning [48, 75, 52], few-shot learning [66], and federated learning [67].

2.3. Mixture of Experts (MoE)

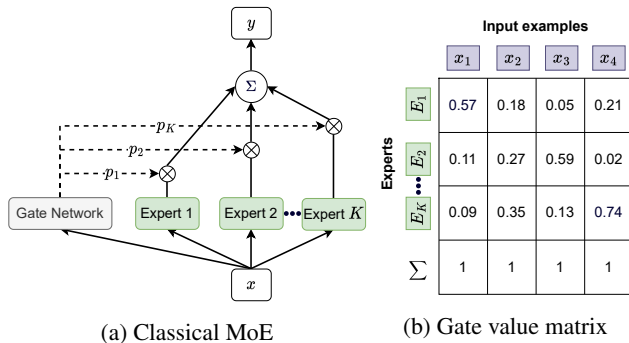


Figure 1: (a) MoE calculates the weighted sum of experts’ outputs. (b) Gate values are determined by the gate network.

MoE was originally proposed by [34, 35] and consists of two main components: experts and a gate network, as shown in Fig. 1. The output of MoE is the weighted sum of experts, with gate values calculated by the gate network on a per-example basis. In recent years, MoE has regained attention as a way to scale up deep learning models and more efficiently harness modern hardware [69, 40, 19, 16, 99, 18]. In this case, sparse MoE is preferred, which routes each example only to the experts with Top-1 or Top-K gate values, instead of all of them.

2.4. Application of Hypernetworks and MoE in DG

As far as we know, no work has applied hypernetworks to solve DG in computer vision. Recently, [81] applied hy-

pernetworks to DG in natural language processing (NLP) and achieved SOTA results on two NLP-related DG tasks.

As for MoE, [41] proposed replacing feed-forward network layer (FFN) of Vision Transformer (ViT) [14] with a sparse mixture of FFN experts to improve DG performance. [27, 94] applied MoE to a task similar to DG, namely domain adaptation [86], but they require domain labels to train an expert for each domain separately. [94] aggregates the outputs of experts via a transformer-based aggregator, but its aggregator is trained with fixed experts and cannot provide probabilities of experts, while HMOE can do this and is more interpretable. In addition, if we regard MoE as a kind of ensemble method, there are some work having the same spirit [53, 13, 97].

3. Method

3.1. Problem Setting

Let \mathcal{X} denote an input space and \mathcal{Y} a target space. A domain S is characterized by a joint distribution P_{XY}^s on $\mathcal{X} \times \mathcal{Y}$. In vanilla DG setting, we have a training set containing M known domains, *i.e.*, $\mathcal{D}_{tr}^V = \{\mathcal{D}^s\}_{s=1}^M$ with $\mathcal{D}^s = \{(x_i^s, y_i^s, d_i^s)\}_{i=1}^{N_s}$ where $(x_i^s, y_i^s) \sim P_{XY}^s$ and d_i^s is the domain index or label. Also consider a test dataset \mathcal{D}_{te} composed of unknown domains different from those of \mathcal{D}_{tr}^V . Vanilla DG aims to train a robust predictor $f : \mathcal{X} \rightarrow \mathcal{Y}$ on \mathcal{D}_{tr}^V to achieve a minimum predictive error on \mathcal{D}_{te} , *i.e.*, $\min_f \mathbb{E}_{(x,y) \sim \mathcal{D}_{te}} [\ell(f(x), y)]$, where ℓ is the loss function.

Our work focuses on the more difficult compound DG, for which the training set $\mathcal{D}_{tr} = \{(x_i, y_i)\}_{i=1}^N$ contains mixed domains and has no domain annotation. However, as demonstrated in [26, 95, 85], intrinsic inter-domain relationships play a key role in obtaining better generalization performance. Therefore, our proposed HMOE is designed to discover latent domains by dividing \mathcal{D}_{tr} into clusters that match human intuition about visual relationships between different domains, and to fully leverage the learned domain information to perform well on unknown domains.

3.2. Overall Architecture

An overview of the HMOE architecture is depicted in Fig. 2a. HMOE processes each input x through two paths: the domain path, which is intended to discover latent domains, and the classifier path, which aims to train a classifier expert for each latent domain.

The classifier path begins with a featurizer h_z to extract high-level features from x , which can be a pretrained network, such as VGG [71], ResNet [30], or ViT [14]. We define a discrete learnable embedding space \mathcal{E} consisting of K embedding vectors $\{e_k \in \mathbb{R}^D\}_{k=1}^K$ (D represents the embedding dimension), each corresponding to a classifier expert. These vectors are fed into a hypernetwork f_h to generate a set of weights $\{\theta_k\}_{k=1}^K$, which further form a set

of experts $\{f_c(:, \theta_k)\}_{k=1}^K$. The output of the featurizer z is passed to these experts to compute their corresponding outputs, that is, $y_k = f_c(z; \theta_k)$.

The domain path begins with a Domain2Vec (D2V) encoder h_v , which transforms x into the embedding space \mathcal{E} and outputs $v \in \mathbb{R}^D$. The output v is then compared with the embedding vectors through a predefined gate function $g(v, \mathcal{E})$, as shown in Fig. 2b, to produce a set of probabilities $\mathbf{p} = \{p_k\}_{k=1}^K$. The final output of HMOE is the weighted sum of the outputs of experts as follows:

$$y = \sum_{k=1}^K p_k y_k = \langle g(h_v(x), \mathcal{E}), [f_c(h_z(x); f_h(e_k))]_{k=1}^K \rangle \quad (1)$$

In the classical MoE, the gate network and experts share the same input. In contrast, the D2V encoder of HMOE takes images as input rather than the featurizer’s extracted features, which mainly contain class-specific information for classification. If we connect the D2V encoder to the featurizer, HMOE risks separating the input space based on semantic categories rather than domain-wise distinction.

3.3. Hypernetworks

We use the hypernetwork f_h taking a vector e as input to generate the weights of the classifier f_c . In our work, both f_h and f_c are MLPs. In a sense, f_c acts as a placeholder computational graph, e can be seen as a conditioning signal, and f_h maps e to a function. The role of f_h is multifaceted: (1) f_h eases latent domain discovery. (2) f_h allows for the use of many experts without significantly increasing the number of parameters. (3) Compared to the classical MoE, f_h offers another way of interaction between experts and the routing mechanism besides the aggregation of experts. (4) As we will see later, by directly taking the D2V encoder as input, f_h enables the generalization of experts beyond aggregation.

3.4. Routing Mechanism

3.4.1 Gate Function

To quantify the responsibilities of experts for each input example and to aggregate experts’ outputs, we need to calculate gate values \mathbf{p} . As shown in Fig. 2b, based on the output of the D2V encoder v and the embedding space \mathcal{E} , we define a gate function $g(v, \mathcal{E})$ to calculate \mathbf{p} as follows:

$$d_k = \|v - e_k\|_2 \quad (2a)$$

$$s_k = -\log(d_k^2 + \epsilon) \quad (2b)$$

$$p_k = \frac{\exp(s_k)}{\sum_{j=1}^K \exp(s_j)} \quad (2c)$$

where ϵ is a small value. The negative logarithm in Eq. (2b) is used to establish a negative correlation between d_k and

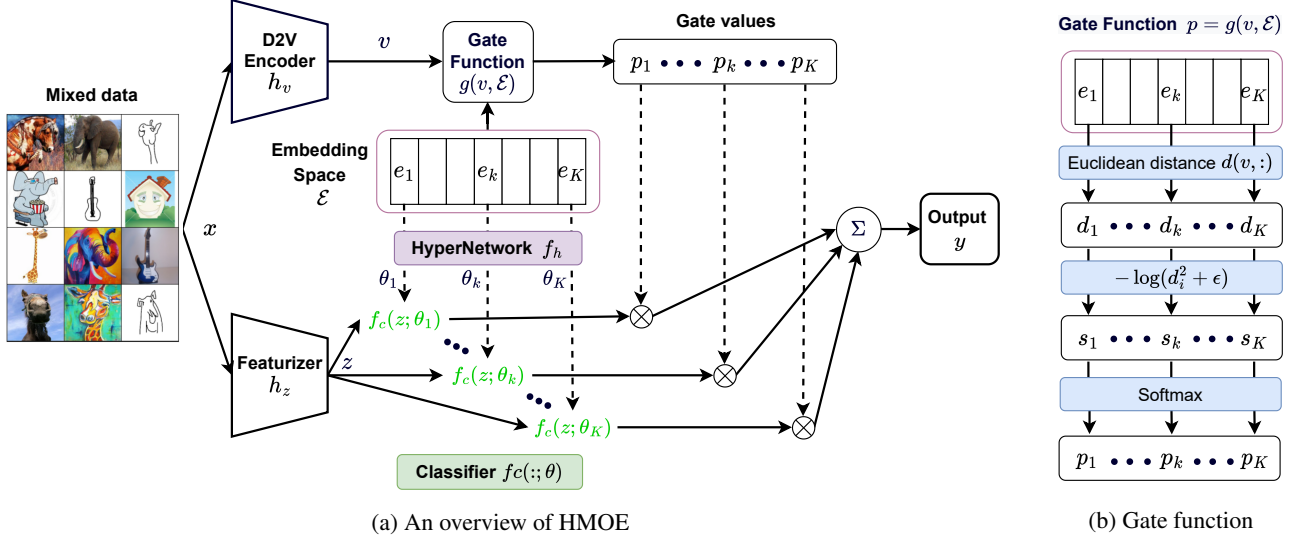


Figure 2: (a) In the upper branch (*i.e.*, the domain path), the input is mapped to the embedding space through the D2V encoder, and gate values are calculated by a predefined gate function. In the lower branch (*i.e.*, the classifier path), the hypernetwork takes embedding vectors as input to create a set of classifiers. The final output is the weighted sum of classifiers’ outputs. (b) The gate function determines gate values based on the distances between the output of the D2V encoder and the embedding vectors. The smaller the distance, the greater the gate value.

p_k (*i.e.*, the smaller d_k , the larger p_k) and to nonlinearly rescale the distance d (*i.e.*, stretch small d and squeeze great d), which makes p less sensitive to large d .

3.4.2 Differentiable Dense-to-Sparse Top-1 Routing

Based on gate values p , the routing mechanism determines where and how to route input examples. A consistent and cohesive routing is crucial to the training stability and convergence of MoE [10]. In order to stabilize the routing and enhance latent domain discovery to capture less obvious domain differences, sparse-gated MoE is preferable. However, the commonly used Top-1 or Top-K functions are not differentiable and cause oscillatory behavior of gate values during training [29]. To overcome this limitation, we propose a differentiable dense-to-sparse Top-1 routing algorithm by introducing an entropy loss on p as follows:

$$\mathcal{L}_{en} = \mathbb{E}_{(x,y) \sim \mathcal{D}_{tr}} [\mathbb{H}(g(h_v(x), \mathcal{E}))] \quad (3)$$

where $\mathbb{H}(\cdot)$ denotes the entropy of a distribution. In practice, we multiply \mathcal{L}_{en} by γ_{en} that linearly increases from 0 to 1 in the first half of training and remains at 1 in the second. Early on, γ_{en} is small, and the distances between v and the embedding vectors are almost the same, leading to a uniform p . Therefore, all experts can be fully trained and gradually become specialized. In the later stages, \mathcal{L}_{en} forces p to become one-hot based on specialized experts.

Due to the negative logarithm in Eq. (2b), the D2V encoder has to move towards one of the embedding vectors

rather than away from the others in order to minimize \mathcal{L}_{en} . As a result, the output of the D2V encoder will converge to \mathcal{E} and become quantized during training.

3.4.3 Expert Load Balancing

Sparse MoE may suffer from an unbalanced expert load, which is problematic if only a small subset of experts are used while the others are left idle. We define the importance of experts as $I(X) = [I_1(X), \dots, I_K(X)]$, where X represents a single batch and $I_k(X)$ is specified as the sum of gate values assigned to the k th expert (*i.e.*, sum the gate value matrix in Fig. 1b along the example dimension). [60] defines a distribution $P = I(X) / \sum I(X)$ and uses the KL-divergence between P and the uniform distribution \mathcal{U} to balance the expert load, which is also used in our work:

$$\mathcal{L}_{kl} = D_{KL}(P \parallel \mathcal{U}) = D_{KL} \left(\frac{I(X)}{\sum I(X)} \parallel \mathcal{U} \right) \quad (4)$$

3.5. Embedding Space

The embedding space \mathcal{E} plays a key role in HMOE. As we can see, the embedding vectors have an effect on both the generation of expert weights and the routing mechanism, thus serving as a bridge to balance these two parts. In addition, these embedding vectors are learnable like the weights of neural networks and attract the D2V encoder during training under the influence of \mathcal{L}_{en} .

3.6. Class-Adversarial Training on D2V

We expect the D2V encoder h_v to contain as little class-specific information as possible, which ensures that HMOE partitions the input space based on domain-wise distinction rather than semantic categories. Inspired by Domain-Adversarial Neural Networks [22], we define an adversarial classifier f_c^{ad} taking v as input and add the following loss to perform class-adversarial training on h_v :

$$\mathcal{L}_{ad} = \mathbb{E}_{(x,y) \sim \mathcal{D}_{tr}} [\ell_{ce}(f_c^{ad}(GRL(v, \lambda_{grl})), y)] \quad (5)$$

where ℓ_{ce} denotes the cross-entropy loss and GRL represents the gradient reversal layer, which acts as an identity function in the forward pass and multiplies the gradient by $-\lambda_{grl}$ in the backward pass. As suggested in [22], we define λ_{grl} as follows:

$$\lambda_{grl} = 2/(1 + \exp(-10 \times pct_{tr})) - 1 \quad (6)$$

where pct_{tr} varies linearly from 0 to 1 during training.

3.7. Semi/supervised Learning on Domains

Due to the probabilistic nature of MoE, given an input x and the corresponding gate values $\mathbf{p} = \{p_k\}_{k=1}^K$, we can interpret p_k as the probability of selecting the k th expert E_k given x , *i.e.*, $p(E_k|x)$. In addition, E_k is thought to be associated with a specific domain S_m . Therefore, we get $p_k = p(E_k|x) = p(S_m|x)$. Consider a dataset with domain labels $\mathcal{D}_d = \{(x_i, d_i)\}_{i=1}^{N_d}$ (class labels are not necessary) with $d_i \in \{1, \dots, M_d\}$, we can make use of \mathcal{D}_d as follows:

$$\mathcal{L}_d = \mathbb{E}_{(x,d) \sim \mathcal{D}_d} [\ell_{ce}(\mathbf{p}, d)] \quad (7)$$

Note that M_d may be smaller than K , but this has no bearing on the calculation of \mathcal{L}_d . In this case, we assume that the first M_d experts are assigned to M_d domains, and the other experts do not have domain information and learn from the data by themselves. If all domain labels are available in the training data, \mathcal{L}_d becomes supervised learning on domains.

3.8. Training and Inference

In addition to the losses mentioned above, the supervised loss on targets is as follows:

$$\mathcal{L}_y = \mathbb{E}_{(x,y) \sim \mathcal{D}_{tr}} [\ell_{ce}(\hat{y}, y)] \quad (8)$$

where \hat{y} is the prediction of HMOE, as calculated by Eq. (1). The final training loss is:

$$\mathcal{L} = \lambda_y \mathcal{L}_y + \lambda_{en} \mathcal{L}_{en} + \lambda_{kl} \mathcal{L}_{kl} + \lambda_{ad} \mathcal{L}_{ad} + \lambda_d \mathcal{L}_d \quad (9)$$

where λ are trade-off hyper-parameters to balance different losses. Generally, λ_y is set to 1 and \mathcal{L}_d is not used for compound DG without domain labels.

For inference, we provide three modes: MIX, MAX, and OOD. MIX refers to the mixture of experts that is calculated by Eq. (1), MAX employs the output of the expert with the highest gate value, and OOD¹ (Out of Domain) uses the output of a classifier whose weights are generated by the hypernetwork directly taking the D2V encoder as input. OOD enables the generalization of experts beyond aggregation.

4. Experiments

This paper focuses on image classification. However, to demonstrate HMOE’s versatility, we also apply it to a toy regression problem to learn a one-dimensional piece-wise function defined on three intervals and HMOE proves effective in identifying discontinuities. Due to space constraints, this toy problem is placed in the **supplementary material**.

Next, we focus on testing HMOE and comparing it with other DG algorithms on DomainBed [26].

4.1. Datasets and Model Evaluation

DomainBed provides a unified codebase to implement and train DG algorithms and integrates commonly used DG-related datasets. In this work, we conduct experiments on Colored MNIST with 3 domains [2], Rotated MNIST with 6 domains [24], PACS with 4 domains [43], VLCS with 4 domains [17], OfficeHome with 4 domains [80], and TerraIncognita with 4 domains [4]. In the **supplementary material**, we give detailed statistics and visualize some samples for each domain of each dataset.

To select models and tune hyper-parameters, DomainBed provides three options, of which we select the training-domain validation that randomly draws 80% from the data of each training domain to form the training set and uses the remaining as the validation set. This option best matches the setting of compound DG without domain labels and access to test domains.

4.2. Implementation Details

For Colored and Rotated MNIST, following [26], we use as the featurizer a four-layer ConvNet (refer to Appendix D.1 of [26]). The D2V encoder h_v consists of two *conv* layers (32 units, 3×3 kernels, ReLU), followed by global average pooling and a fully-connected (fc) layer to map to the embedding dimension D .

For other datasets, we use ResNet-50² pretrained on ImageNet [11] as the featurizer and freeze all batch normalization layers. The D2V encoder h_v cascades 3 *conv* layers (64-128-256 units, stride 2, 4×4 kernels, ReLU), two residual blocks (each has 2 *conv* layers with 256 units, 3×3 kernels, ReLU), and a 3×3 *conv* layer with D units followed

¹The OOD inference can be efficiently implemented using PyTorch-based JAX-like library, *functorch*.

²For a fair comparison with other DG algorithms, we use the pretrained ResNet-50 of IMAGENET1K-V1 in PyTorch, although V2 is better.

by global average pooling. We use Instance Normalization [77] with learnable affine parameters before all ReLU of h_v .

For all datasets, the classifier f_c is a fc layer whose input size is the featurizer’s output size (128 for ConvNet and 2048 for ResNet-50) and output size is the number of classes. The hypernetwork f_h is a five-layer MLP with 256-128-64-32 hidden units and SiLU [31] except the output layer, and its input size is D and output size is the total number of learnable parameters (*i.e.*, weights and biases) of f_c . In addition, we use the hyperfan method proposed by [8] to initialize f_h . If \mathcal{L}_{ad} is used, the adversarial classifier is a three-layer MLP with 256 hidden units and ReLU except the output layer, and its input size is D and output size is the number of classes. We set $D = 32$ and initialize embedding vectors using the standard normal distribution.

We define three HMOE variants based on the number of embedding vectors K and whether domain labels are used: (1) **HMOE-DL**: Domain labels of \mathcal{D}_{tr} are provided. In this case, we only use \mathcal{L}_y and \mathcal{L}_d with $\lambda_y = \lambda_d = 1$ and discard other losses, and K is the number of training domains per dataset. (2) **HMOE-DN**: Domain numbers are known but domain labels. In this case, K is the number of training domains per dataset. We use \mathcal{L}_y , \mathcal{L}_{en} , \mathcal{L}_{kl} , and \mathcal{L}_{ad} with $\lambda_y = \lambda_{en} = \lambda_{kl} = 1$ and $\lambda_{ad} = 0.01$. (3) **HMOE-ND**: No domain information is available and we use a fixed $K = 5$. The setting of losses is the same as in HMOE-DN.

DomainBed trains all DG algorithms with Adam for 5,000 iterations. For Colored and Rotated MNIST / other datasets, the learning rate is 0.001 / $5e-5$, the batch size is 64 / $32 \times$ number of training domains, and models are evaluated on the validation set every 100 / 300 iterations. Each experiment uses one domain of a dataset as the test domain and trains algorithms on the others, which is repeated 3 times with different random seeds. The average accuracy over 3 replicates is reported. In addition, we do not tune HMOE’s hyper-parameters and use the settings mentioned above consistently. Other DG algorithms also use the default settings predefined in DomainBed. All experiments are performed on PyTorch using a A5000 GPU.

4.3. Results

We use the up-to-date domain generalization benchmark on DomainBed, and the comparison of HMOE (3 variants and 3 inference modes) with other DG algorithms is shown in Tab. 1, where the best results are underlined. ERM means the vanilla supervised learning that just fine-tunes ResNet-50 on mixed data, also called DeepAll in some papers and serving as a performance baseline. We report the average accuracy of all test domains for each dataset. Refer to the **supplementary material** for detailed results.

For Colored and Rotated MNIST, all algorithms exhibit similar performance, except the impressive results of ARM. HMOE achieves SOTA results on PACS and TerraIncognita,

which well demonstrates its effectiveness. However, ERM outperforms HMOE and most DG algorithms for VLCS and OfficeHome. VLCS contains real camera photos, and its domain shift is mainly caused by changes in scene and perspective. We find that the visual differences between different domains of VLCS are subtle. In this case, forcing to reduce or model domain discrepancy may cause or aggravate overfitting. For OfficeHome, this is also the case. Interestingly, HMOE-DL is inferior to HMOE-DN/ND in most cases, which implies that HMOE works better using its own learned domain information than using given domain labels. We find that latent domains discovered by HMOE are more human-intuitive than original domain labels (Section 4.4).

Fig. 3 shows the supervised loss on domains of HMOE-DL \mathcal{L}_d w.r.t. iterations, which fails to decrease quickly for OfficeHome and VLCS. This implies that the information of domain labels is not well absorbed and seems to be incompatible with HMOE.

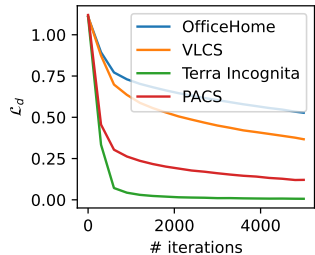


Figure 3: Avg \mathcal{L}_d per dataset

HMOE-DN / ND are basically tied in terms of performance. For three inference modes, MAX and OOD are competitive with MIX in most cases and can be used to sacrifice a little accuracy for efficiency in practice because MAX and OOD are more computationally efficient without computing all experts like MIX.

4.4. Latent Domain Discovery

We use t-SNE [78] to visualize the output of the D2V encoder, as shown in Fig. 4. We can see that HMOE effectively partitions the mixed data into a number of clusters, each centered around an embedding vector. As expected, the output of the D2V encoder converges to embedding vectors. For PACS (Fig. 4a), the training domains are well separated. Some cartoon images look quite artistic and are classified as art. In addition, test photo samples are projected into the art cluster, suggesting that the D2V encoder should capture some semantics about latent domains since photo is closest to art. If we increase the number of embedding vectors K to 5, cartoon and sketch clusters are split into two sub-clusters, as shown in Fig. 4b. For TerraIncognita (Fig. 4c), the dots of the same color are largely clustered together. The training domains are to some extent separated, although L38 and L43 are partially mixed. The test domain L46 seems to be more similar to L100. For OfficeHome (Fig. 4d), the training domains are mixed within each cluster, indicating a conflict between domain labels and inferred domains. This also explains why \mathcal{L}_d cannot be significantly reduced for OfficeHome in Fig. 3.

To intuitively understand how HMOE distinguishes be-

Algorithm		ColoredMNIST	RotatedMNIST	VLCS	PACS	OfficeHome	TerraIncognita
<i>w/ Domain Labels</i>							
IRM [2]		52.0 ± 0.1	97.7 ± 0.1	78.5 ± 0.5	83.5 ± 0.8	64.3 ± 2.2	47.6 ± 0.8
GroupDRO [65]		52.1 ± 0.0	98.0 ± 0.0	76.7 ± 0.6	84.4 ± 0.8	66.0 ± 0.7	43.2 ± 1.1
Mixup [87]		52.1 ± 0.2	98.0 ± 0.1	77.4 ± 0.6	84.6 ± 0.6	68.1 ± 0.3	47.9 ± 0.8
MLDG [42]		51.5 ± 0.1	97.9 ± 0.0	77.2 ± 0.4	84.9 ± 1.0	66.8 ± 0.6	47.7 ± 0.9
CORAL [74]		51.5 ± 0.1	98.0 ± 0.1	78.8 ± 0.6	86.2 ± 0.3	68.7 ± 0.3	47.6 ± 1.0
MMD [45]		51.5 ± 0.2	97.9 ± 0.0	77.5 ± 0.9	84.6 ± 0.5	66.3 ± 0.1	42.2 ± 1.6
DANN [22]		51.5 ± 0.3	97.8 ± 0.1	78.6 ± 0.4	83.6 ± 0.4	65.9 ± 0.6	46.7 ± 0.5
CDANN [47]		51.7 ± 0.1	97.9 ± 0.1	77.5 ± 0.1	82.6 ± 0.9	65.8 ± 1.3	45.8 ± 1.6
MTL [5]		51.4 ± 0.1	97.9 ± 0.0	77.2 ± 0.4	84.6 ± 0.5	66.4 ± 0.5	45.6 ± 1.2
ARM [92]		56.2 ± 0.2	98.2 ± 0.1	77.6 ± 0.3	85.1 ± 0.4	64.8 ± 0.3	45.5 ± 0.3
VREx [39]		51.8 ± 0.1	97.9 ± 0.1	78.3 ± 0.2	84.9 ± 0.6	66.4 ± 0.6	46.4 ± 0.6
HMOE-DL	MIX	51.6 ± 0.1	97.3 ± 0.1	76.7 ± 0.4	83.5 ± 0.5	64.7 ± 0.2	45.0 ± 0.8
	MAX	51.7 ± 0.1	97.0 ± 0.0	77.6 ± 0.3	83.9 ± 0.3	63.2 ± 0.1	43.2 ± 1.5
	OOD	51.7 ± 0.2	97.4 ± 0.1	76.8 ± 0.9	84.5 ± 0.3	63.7 ± 0.2	44.0 ± 0.9
<i>w/o Domain Labels</i>							
ERM [79]		51.5 ± 0.1	98.0 ± 0.0	77.5 ± 0.4	85.5 ± 0.2	66.5 ± 0.3	46.1 ± 1.8
RSC [32]		51.7 ± 0.2	97.6 ± 0.1	77.1 ± 0.5	85.2 ± 0.9	65.5 ± 0.9	46.6 ± 1.0
SagNet [57]		51.7 ± 0.0	98.0 ± 0.0	77.8 ± 0.5	86.3 ± 0.2	68.1 ± 0.1	48.6 ± 1.0
HMOE-DN	MIX	51.9 ± 0.1	97.5 ± 0.1	76.8 ± 0.5	84.8 ± 0.6	65.4 ± 0.4	48.7 ± 1.3
	MAX	51.9 ± 0.1	97.4 ± 0.0	76.6 ± 0.4	85.1 ± 0.5	65.4 ± 0.3	49.5 ± 1.0
	OOD	51.9 ± 0.2	97.5 ± 0.0	75.8 ± 0.2	84.9 ± 0.7	65.3 ± 0.1	48.4 ± 0.9
HMOE-ND	MIX	51.6 ± 0.0	97.5 ± 0.1	76.6 ± 0.2	84.5 ± 0.5	65.5 ± 0.3	48.4 ± 1.4
	MAX	51.7 ± 0.1	97.4 ± 0.0	76.8 ± 0.2	86.6 ± 0.6	65.5 ± 0.3	45.0 ± 1.7
	OOD	51.7 ± 0.1	97.5 ± 0.0	76.7 ± 0.5	87.0 ± 0.2	65.6 ± 0.1	47.1 ± 1.1

Table 1: Domain generalization results on DomainBed

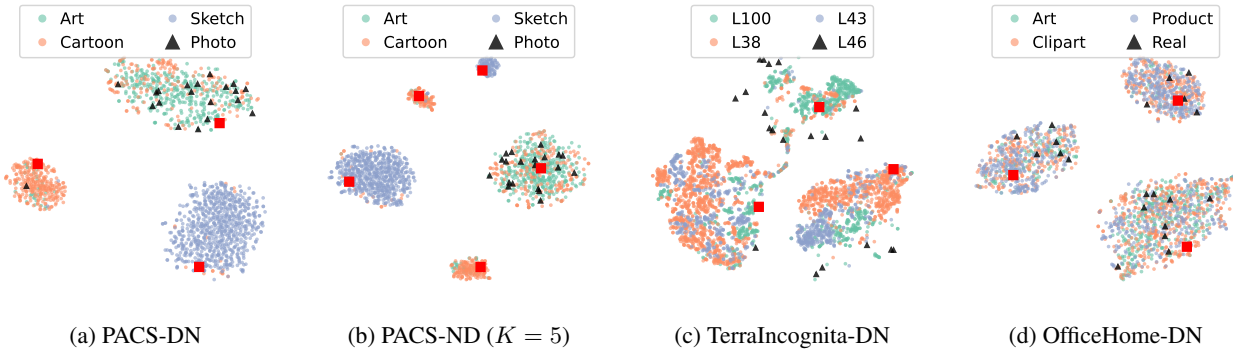


Figure 4: The t-SNE visualization of the output of the D2V encoder. The suffixes in captions (DN and ND) represent HMOE-DN / ND, red squares are embedding vectors, black triangles are 20 samples randomly drawn from the test domain, and other dots are training domains. The silhouette coefficients are 0.73, 0.72, 0.54 and 0.63 for Figs. 4a to 4d, respectively.

tween domains, we visualize some samples to compare domain labels and HMOE’s clusters, as shown in Fig. 5. HMOE seems to partition TerraIncognita based on illumination and OfficeHome based on background complexity, which more matches human intuition than domain labels.

After the above analysis, we conclude that the success of HMOE, *e.g.*, SOTA on PACS and TerraIncognita, can be attributed to its ability to self-learn more reasonable and informative domain knowledge and use it efficiently.

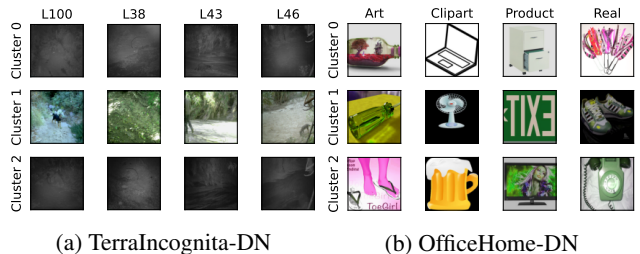


Figure 5: Compare domain labels and HMOE’s clusters

4.5. Ablation Study

In this section, we conduct an ablation study to analyze the contribution of each component of HMOE. The results are shown in Tab. 2, which reports the average accuracy of three inference modes. We employ the silhouette coefficient (SC) to quantitatively evaluate the HMOE’s clustering based on both the compactness and separation of clusters. SC ranges from -1 (poor) to 1 (good). We use gate values to identify clusters and the output of the D2V encoder to measure the distance between them.

Name	\mathcal{L}_{en}	\mathcal{L}_{kl}	\mathcal{L}_{ad}	VLCS	PACS	Office	TerraInc	Avg. SC
H1	-	-	-	76.1	83.2	64.2	46.8	0.37
H2	-	-	✓	76.8	84.2	64.7	47.5	0.27
H3	✓	-	-	76.3	81.8	63.7	43.4	Collapse
H4	✓	-	✓	75.9	82.1	62.2	44.1	Collapse
H5	✓	✓	-	76.0	84.0	64.2	47.0	0.65
H6	✓	✓	✓	76.4	84.9	65.4	48.9	0.60

Table 2: Ablation study for HMOE-DN (avg. accuracy of MIX, MAX and OOD is reported, ✓ means the corresponding loss is used, and SC denotes the silhouette coefficient.)

Top-1 routing \mathcal{L}_{en} and expert load balancing \mathcal{L}_{kl}

Tab. 2 shows that the joint use of \mathcal{L}_{en} and \mathcal{L}_{kl} leads to better clustering with greater SC and promotes latent domain discovery. Without them, HMOE divides the data through MoE’s intrinsic soft partitioning. H6 outperforms H2 in most cases, which could indicate that better clustering helps improve the DG performance. However, H1 and H5 have comparable performance, probably due to the absence of \mathcal{L}_{ad} . We find that \mathcal{L}_{en} without \mathcal{L}_{kl} suffers from the learning collapse problem, *i.e.*, some embedding vectors collapse together and the D2V encoder outputs similar values. An example is shown Fig. 6. This shows the importance of \mathcal{L}_{kl} .

Class-adversarial training \mathcal{L}_{ad} helps improve accuracy in most cases, verifying the necessity of removing class-specific information from the D2V encoder. H2 and H6 have smaller SC than H1 and H5, respectively, which is logical as class information can still be used by H1 and H5 for clustering, but is somewhat removed for H2 and H6 via \mathcal{L}_{ad} .

4.6. More Empirical Analysis

More embedding vectors We further increase K to 8 and find that HMOE also suffers from the learning collapse problem, as shown in Fig. 6. When embedding vectors are much more than needed, HMOE has difficulties in how to correctly assign the data to different experts.

Train HMOE using OOD As mentioned earlier, hypernetworks f_h associate experts with vectors, enabling the exploration of experts’ similarities in a low-dimensional vector space and facilitating latent domain discovery. To verify

this, we use OOD (*i.e.*, f_h takes the D2V encoder h_v as input) to train HMOE, which means that each input can have its own expert, instead of selecting from a few given experts. This involves minimizing the following loss:

$$\mathcal{L}_{ood} = \mathbb{E}_{(x,y) \sim \mathcal{D}_{tr}} [\ell_{ce}(f_c(h_z(x); f_h(h_v(x))), y)] \quad (10)$$

After training, the D2V encoder is also able to distinguish between different domains, as shown in Fig. 7. This nicely demonstrates the role of hypernetworks in learning and capturing semantic similarities across domains.

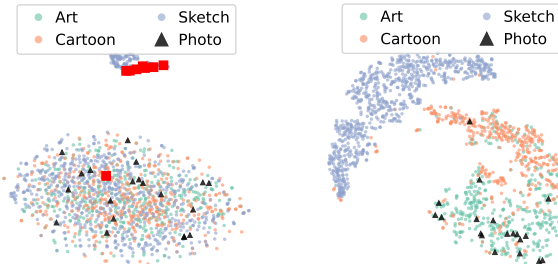


Figure 6: Learning collapse Figure 7: Train HMOE using OOD for PACS with $K = 8$

Use Swin Transformer as featurizer [72, 41] investigate the impact of the backbone architecture (*i.e.*, the featurizer for HMOE) on DG, and [41] found that the transformer-based backbone outperforms the CNN-based counterpart. Motivated by this, we replace ResNet-50 with Swin Transformer [50] (the pretrained small version in PyTorch and its output size is 768) as the featurizer of HMOE-DN. The results are shown in Tab. 3, where ERM just fine-tunes Swin Transformer and we report the MIX mode of HMOE-DN. Tab. 3 is clearly superior to Tab. 1. HMOE-DN outperforms ERM on PACS and TerraIncognita and they are comparable on the other two datasets.

	VLCS	PACS	OfficeHome	TerraIncognita
ERM [79]	79.8	86.9	76.0	54.1
HMOE-DN	79.6	87.6	76.1	55.3

Table 3: Use Swin Transformer as featurizer of HMOE-DN

5. Conclusion

This paper presents a novel DG method, HMOE, which does not require domain labels, enables latent domain discovery, and provides excellent interpretability. HMOE uses the framework of Mixture of Experts (MoE) to solve the DG problem and employs hypernetworks to generate the weights of experts. Compared to other DG methods requiring domain labels, HMOE shows competitive performance and achieves SOTA results on the PACS and TerraIncognita datasets. It is worth mentioning that the discovery and utilization of domain information are jointly undertaken for HMOE, rather than in stages like other related work.

However, it also remains unclear how to effectively determine an appropriate number of experts or embedding vectors to fully explore domain information while avoiding the learning collapse. A promising solution that we will explore in future work is to use tree-structured hierarchical MoE to discover hierarchical domain knowledge, where each level contains only a number of experts but the number of multi-level inferred domains grows exponentially.

Finally, HMOE is versatile and scalable, and it should also be applicable to a wide range of problems beyond the scope of DG that are troubled by heterogeneous patterns.

References

- [1] Kartik Ahuja, Ethan Caballero, Dinghuai Zhang, Jean-Christophe Gagnon-Audet, Yoshua Bengio, Ioannis Mitliagkas, and Irina Rish. Invariance principle meets information bottleneck for out-of-distribution generalization. *Advances in Neural Information Processing Systems*, 34:3438–3450, 2021. [2](#)
- [2] Martin Arjovsky, Léon Bottou, Ishaan Gulrajani, and David Lopez-Paz. Invariant risk minimization. *arXiv preprint arXiv:1907.02893*, 2019. [2](#), [5](#), [7](#), [3](#), [4](#)
- [3] Yogesh Balaji, Swami Sankaranarayanan, and Rama Chelappa. Metareg: Towards domain generalization using meta-regularization. *Advances in neural information processing systems*, 31, 2018. [2](#)
- [4] Sara Beery, Grant Van Horn, and Pietro Perona. Recognition in terra incognita. In *Proceedings of the European Conference on Computer Vision (ECCV)*, pages 456–473, 2018. [5](#), [2](#)
- [5] Gilles Blanchard, Aniket Anand Deshmukh, Ürun Dogan, Gyemin Lee, and Clayton Scott. Domain generalization by marginal transfer learning. *The Journal of Machine Learning Research*, 22(1):46–100, 2021. [1](#), [2](#), [7](#), [3](#), [4](#), [5](#)
- [6] Dhanajit Brahma, Vinay Kumar Verma, and Piyush Rai. Hypernetworks for Continual Semi-Supervised Learning. *arXiv preprint arXiv:2110.01856*, 2021. [2](#)
- [7] Fabio M. Carlucci, Antonio D’Innocente, Silvia Bucci, Barbara Caputo, and Tatiana Tommasi. Domain generalization by solving jigsaw puzzles. In *Proceedings of the IEEE/CVF Conference on Computer Vision and Pattern Recognition*, pages 2229–2238, 2019. [2](#)
- [8] Oscar Chang, Lampros Flokas, and Hod Lipson. Principled weight initialization for hypernetworks. In *International Conference on Learning Representations*, 2019. [6](#)
- [9] Chaoqi Chen, Jiongcheng Li, Xiaoguang Han, Xiaoqing Liu, and Yizhou Yu. Compound Domain Generalization via Meta-Knowledge Encoding. In *Proceedings of the IEEE/CVF Conference on Computer Vision and Pattern Recognition*, pages 7119–7129, 2022. [1](#), [2](#)
- [10] Damai Dai, Li Dong, Shuming Ma, Bo Zheng, Zhifang Sui, Baobao Chang, and Furu Wei. StableMoE: Stable routing strategy for mixture of experts. *arXiv preprint arXiv:2204.08396*, 2022. [4](#)
- [11] Jia Deng, Wei Dong, Richard Socher, Li-Jia Li, Kai Li, and Li Fei-Fei. Imagenet: A large-scale hierarchical image database. In *2009 IEEE Conference on Computer Vision and Pattern Recognition*, pages 248–255. Ieee, 2009. [5](#)
- [12] Aniket Anand Deshmukh, Yunwen Lei, Srinagesh Sharma, Ürun Dogan, James W. Cutler, and Clayton Scott. A generalization error bound for multi-class domain generalization. *arXiv preprint arXiv:1905.10392*, 2019. [1](#)
- [13] Antonio D’Innocente and Barbara Caputo. Domain generalization with domain-specific aggregation modules. In *German Conference on Pattern Recognition*, pages 187–198. Springer, 2018. [3](#)
- [14] Alexey Dosovitskiy, Lucas Beyer, Alexander Kolesnikov, Dirk Weissenborn, Xiaohua Zhai, Thomas Unterthiner, Mostafa Dehghani, Matthias Minderer, Georg Heigold, and Sylvain Gelly. An image is worth 16x16 words: Transformers for image recognition at scale. *arXiv preprint arXiv:2010.11929*, 2020. [3](#)
- [15] Qi Dou, Daniel Coelho de Castro, Konstantinos Kamnitsas, and Ben Glocker. Domain generalization via model-agnostic learning of semantic features. *Advances in Neural Information Processing Systems*, 32, 2019. [2](#)
- [16] Nan Du, Yanping Huang, Andrew M. Dai, Simon Tong, Dmitry Lepikhin, Yuanzhong Xu, Maxim Krikun, Yanqi Zhou, Adams Wei Yu, and Orhan Firat. Glam: Efficient scaling of language models with mixture-of-experts. In *International Conference on Machine Learning*, pages 5547–5569. PMLR, 2022. [2](#)
- [17] Chen Fang, Ye Xu, and Daniel N. Rockmore. Unbiased metric learning: On the utilization of multiple datasets and web images for softening bias. In *Proceedings of the IEEE International Conference on Computer Vision*, pages 1657–1664, 2013. [5](#), [2](#)
- [18] William Fedus, Jeff Dean, and Barret Zoph. A review of sparse expert models in deep learning. *arXiv preprint arXiv:2209.01667*, 2022. [2](#)
- [19] William Fedus, Barret Zoph, and Noam Shazeer. *Switch Transformers: Scaling to Trillion Parameter Models with Simple and Efficient Sparsity*. 2021. [2](#)
- [20] Chuang Gan, Tianbao Yang, and Boqing Gong. Learning attributes equals multi-source domain generalization. In *Proceedings of the IEEE Conference on Computer Vision and Pattern Recognition*, pages 87–97, 2016. [2](#)
- [21] Yaroslav Ganin and Victor Lempitsky. Unsupervised domain adaptation by backpropagation. In *International Conference on Machine Learning*, pages 1180–1189. PMLR, 2015. [2](#)
- [22] Yaroslav Ganin, Evgeniya Ustinova, Hana Ajakan, Pascal Germain, Hugo Larochelle, François Laviolette, Mario Marchand, and Victor Lempitsky. Domain-adversarial training of neural networks. *The journal of machine learning research*, 17(1):2096–2030, 2016. [2](#), [5](#), [7](#), [3](#), [4](#)
- [23] Muhammad Ghifary, David Balduzzi, W. Bastiaan Kleijn, and Mengjie Zhang. Scatter component analysis: A unified framework for domain adaptation and domain generalization. *IEEE transactions on pattern analysis and machine intelligence*, 39(7):1414–1430, 2016. [2](#)
- [24] Muhammad Ghifary, W. Bastiaan Kleijn, Mengjie Zhang, and David Balduzzi. Domain generalization for object recognition with multi-task autoencoders. In *Proceedings of the IEEE International Conference on Computer Vision*, pages 2551–2559, 2015. [2](#), [5](#)
- [25] Rui Gong, Wen Li, Yuhua Chen, and Luc Van Gool. Dlow: Domain flow for adaptation and generalization. In *Proceedings of the IEEE/CVF Conference on Computer Vision and Pattern Recognition*, pages 2477–2486, 2019. [2](#)
- [26] Ishaan Gulrajani and David Lopez-Paz. In search of lost domain generalization. *arXiv preprint arXiv:2007.01434*, 2020. [1](#), [2](#), [3](#), [5](#)
- [27] Jiang Guo, Darsh J. Shah, and Regina Barzilay. Multi-source domain adaptation with mixture of experts. *arXiv preprint arXiv:1809.02256*, 2018. [1](#), [3](#)
- [28] David Ha, Andrew Dai, and Quoc V. Le. Hypernetworks. *arXiv preprint arXiv:1609.09106*, 2016. [1](#), [2](#)

- [29] Hussein Hazimeh, Zhe Zhao, Aakanksha Chowdhery, Maheswaran Sathiamoorthy, Yihua Chen, Rahul Mazumder, Lichan Hong, and Ed Chi. Dselect-k: Differentiable selection in the mixture of experts with applications to multi-task learning. *Advances in Neural Information Processing Systems*, 34:29335–29347, 2021. 4
- [30] Kaiming He, Xiangyu Zhang, Shaoqing Ren, and Jian Sun. Deep residual learning for image recognition. In *Proceedings of the IEEE Conference on Computer Vision and Pattern Recognition*, pages 770–778, 2016. 3
- [31] Dan Hendrycks and Kevin Gimpel. Gaussian error linear units (gelus). *arXiv preprint arXiv:1606.08415*, 2016. 6, 1
- [32] Zeyi Huang, Haohan Wang, Eric P. Xing, and Dong Huang. Self-challenging improves cross-domain generalization. In *European Conference on Computer Vision*, pages 124–140. Springer, 2020. 2, 7, 3, 4, 5
- [33] Maximilian Ilse, Jakub M Tomczak, Christos Louizos, and Max Welling. Diva: Domain invariant variational autoencoders. In *Medical Imaging with Deep Learning*, pages 322–348. PMLR, 2020. 2
- [34] Robert A. Jacobs, Michael I. Jordan, Steven J. Nowlan, and Geoffrey E. Hinton. Adaptive mixtures of local experts. *Neural computation*, 3(1):79–87, 1991. 1, 2
- [35] Michael I. Jordan and Robert A. Jacobs. Hierarchical mixtures of experts and the EM algorithm. *Neural computation*, 6(2):181–214, 1994. 1, 2
- [36] Aditya Khosla, Tinghui Zhou, Tomasz Malisiewicz, Alexei A. Efros, and Antonio Torralba. Undoing the damage of dataset bias. In *European Conference on Computer Vision*, pages 158–171. Springer, 2012. 2
- [37] Daehee Kim, Youngjun Yoo, Seunghyun Park, Jinkyu Kim, and Jaekoo Lee. Selfreg: Self-supervised contrastive regularization for domain generalization. In *Proceedings of the IEEE/CVF International Conference on Computer Vision*, pages 9619–9628, 2021. 2
- [38] Diederik P Kingma and Jimmy Ba. Adam: A method for stochastic optimization. *arXiv preprint arXiv:1412.6980*, 2014. 1
- [39] David Krueger, Ethan Caballero, Joern-Henrik Jacobsen, Amy Zhang, Jonathan Binas, Dinghui Zhang, Remi Le Priol, and Aaron Courville. Out-of-distribution generalization via risk extrapolation (rex). In *International Conference on Machine Learning*, pages 5815–5826. PMLR, 2021. 2, 7, 3, 4, 5
- [40] Dmitry Lepikhin, HyoukJoong Lee, Yuanzhong Xu, Dehao Chen, Orhan Firat, Yanping Huang, Maxim Krikun, Noam Shazeer, and Zhifeng Chen. Gshard: Scaling giant models with conditional computation and automatic sharding. *arXiv preprint arXiv:2006.16668*, 2020. 2
- [41] Bo Li, Jingkan Yang, Jiawei Ren, Yezhen Wang, and Ziwei Liu. Sparse Fusion Mixture-of-Experts are Domain Generalizable Learners. *arXiv preprint arXiv:2206.04046*, 2022. 3, 8
- [42] Da Li, Yongxin Yang, Yi-Zhe Song, and Timothy M. Hospedales. Learning to generalize: Meta-learning for domain generalization. In *Proceedings of the AAAI Conference on Artificial Intelligence*, volume 32, 2018. 2, 7, 3, 4, 5
- [43] Da Li, Yongxin Yang, Yi-Zhe Song, and Timothy M. Hospedales. Deeper, broader and artier domain generalization. In *Proceedings of the IEEE International Conference on Computer Vision*, pages 5542–5550, 2017. 5, 2
- [44] Da Li, Jianshu Zhang, Yongxin Yang, Cong Liu, Yi-Zhe Song, and Timothy M. Hospedales. Episodic training for domain generalization. In *Proceedings of the IEEE/CVF International Conference on Computer Vision*, pages 1446–1455, 2019. 2
- [45] Haoliang Li, Sinno Jialin Pan, Shiqi Wang, and Alex C Kot. Domain generalization with adversarial feature learning. In *Proceedings of the IEEE Conference on Computer Vision and Pattern Recognition*, pages 5400–5409, 2018. 2, 7, 3, 4, 5
- [46] Pan Li, Da Li, Wei Li, Shaogang Gong, Yanwei Fu, and Timothy M. Hospedales. A simple feature augmentation for domain generalization. In *Proceedings of the IEEE/CVF International Conference on Computer Vision*, pages 8886–8895, 2021. 2
- [47] Ya Li, Xinmei Tian, Mingming Gong, Yajing Liu, Tongliang Liu, Kun Zhang, and Dacheng Tao. Deep domain generalization via conditional invariant adversarial networks. In *Proceedings of the European Conference on Computer Vision (ECCV)*, pages 624–639, 2018. 2, 7, 3, 4, 5
- [48] Xi Lin, Zhiyuan Yang, Qingfu Zhang, and Sam Kwong. Controllable pareto multi-task learning. *arXiv preprint arXiv:2010.06313*, 2020. 2
- [49] Alexander H. Liu, Yen-Cheng Liu, Yu-Ying Yeh, and Yu-Chiang Frank Wang. A unified feature disentangler for multi-domain image translation and manipulation. *Advances in neural information processing systems*, 31, 2018. 2
- [50] Ze Liu, Yutong Lin, Yue Cao, Han Hu, Yixuan Wei, Zheng Zhang, Stephen Lin, and Baining Guo. Swin transformer: Hierarchical vision transformer using shifted windows. In *Proceedings of the IEEE/CVF International Conference on Computer Vision*, pages 10012–10022, 2021. 8
- [51] Jonathan Lorraine and David Duvenaud. Stochastic hyperparameter optimization through hypernetworks. *arXiv preprint arXiv:1802.09419*, 2018. 2
- [52] Rabeeh Karimi Mahabadi, Sebastian Ruder, Mostafa Dehghani, and James Henderson. Parameter-efficient multi-task fine-tuning for transformers via shared hypernetworks. *arXiv preprint arXiv:2106.04489*, 2021. 2
- [53] Massimiliano Mancini, Samuel Rota Buló, Barbara Caputo, and Elisa Ricci. Best sources forward: Domain generalization through source-specific nets. In *2018 25th IEEE International Conference on Image Processing (ICIP)*, pages 1353–1357. IEEE, 2018. 3
- [54] Toshihiko Matsuura and Tatsuya Harada. Domain generalization using a mixture of multiple latent domains. In *Proceedings of the AAAI Conference on Artificial Intelligence*, volume 34, pages 11749–11756, 2020. 2
- [55] Saied Motiian, Marco Piccirilli, Donald A. Adjeroh, and Gianfranco Doretto. Unified deep supervised domain adaptation and generalization. In *Proceedings of the IEEE International Conference on Computer Vision*, pages 5715–5725, 2017. 2

- [56] Krikamol Muandet, David Balduzzi, and Bernhard Schölkopf. Domain generalization via invariant feature representation. In *International Conference on Machine Learning*, pages 10–18. PMLR, 2013. 1, 2
- [57] Hyeonseob Nam, HyunJae Lee, Jongchan Park, Wonjun Yoon, and Donggeun Yoo. Reducing domain gap by reducing style bias. In *Proceedings of the IEEE/CVF Conference on Computer Vision and Pattern Recognition*, pages 8690–8699, 2021. 2, 7, 3, 4, 5
- [58] Aviv Navon, Aviv Shamsian, Gal Chechik, and Ethan Fetaya. Learning the pareto front with hypernetworks. *arXiv preprint arXiv:2010.04104*, 2020. 2
- [59] Sinno Jialin Pan, Ivor W. Tsang, James T. Kwok, and Qiang Yang. Domain adaptation via transfer component analysis. *IEEE transactions on neural networks*, 22(2):199–210, 2010. 2
- [60] Svetlana Pavlitskaya, Christian Hubschneider, Lukas Struppek, and J. Marius Zöllner. Balancing Expert Utilization in Mixture-of-Experts Layers Embedded in CNNs. *arXiv preprint arXiv:2204.10598*, 2022. 4
- [61] Xingchao Peng, Qinxun Bai, Xide Xia, Zijun Huang, Kate Saenko, and Bo Wang. Moment matching for multi-source domain adaptation. In *Proceedings of the IEEE/CVF International Conference on Computer Vision*, pages 1406–1415, 2019. 2
- [62] Xingchao Peng, Zijun Huang, Ximeng Sun, and Kate Saenko. Domain agnostic learning with disentangled representations. In *International Conference on Machine Learning*, pages 5102–5112. PMLR, 2019. 2
- [63] Fengchun Qiao, Long Zhao, and Xi Peng. Learning to learn single domain generalization. In *Proceedings of the IEEE/CVF Conference on Computer Vision and Pattern Recognition*, pages 12556–12565, 2020. 2
- [64] Alexandre Rame, Corentin Dancette, and Matthieu Cord. Fishr: Invariant gradient variances for out-of-distribution generalization. In *International Conference on Machine Learning*, pages 18347–18377. PMLR, 2022. 2
- [65] Shiori Sagawa, Pang Wei Koh, Tatsunori B. Hashimoto, and Percy Liang. Distributionally Robust Neural Networks for Group Shifts: On the Importance of Regularization for Worst-Case Generalization, Apr. 2020. 2, 7, 3, 4, 5
- [66] Marcin Sendera, Marcin Przewięźlikowski, Konrad Karanowski, Maciej Zięba, Jacek Tabor, and Przemysław Spurek. Hypershot: Few-shot learning by kernel hypernetworks. *arXiv preprint arXiv:2203.11378*, 2022. 2
- [67] Aviv Shamsian, Aviv Navon, Ethan Fetaya, and Gal Chechik. Personalized federated learning using hypernetworks. In *International Conference on Machine Learning*, pages 9489–9502. PMLR, 2021. 2
- [68] Shiv Shankar, Vihari Piratla, Soumen Chakrabarti, Siddhartha Chaudhuri, Preethi Jyothi, and Sunita Sarawagi. Generalizing across domains via cross-gradient training. *arXiv preprint arXiv:1804.10745*, 2018. 2
- [69] Noam Shazeer, Azalia Mirhoseini, Krzysztof Maziarz, Andy Davis, Quoc Le, Geoffrey Hinton, and Jeff Dean. Outrageously large neural networks: The sparsely-gated mixture-of-experts layer. *arXiv preprint arXiv:1701.06538*, 2017. 2
- [70] Yuge Shi, Jeffrey Seely, Philip HS Torr, N. Siddharth, Awni Hannun, Nicolas Usunier, and Gabriel Synnaeve. Gradient matching for domain generalization. *arXiv preprint arXiv:2104.09937*, 2021. 2
- [71] Karen Simonyan and Andrew Zisserman. Very deep convolutional networks for large-scale image recognition. *arXiv preprint arXiv:1409.1556*, 2014. 3
- [72] Sarath Sivaprasad, Akshay Goindani, Vaibhav Garg, and Vineet Gandhi. Reappraising Domain Generalization in Neural Networks. *arXiv preprint arXiv:2110.07981*, 2021. 8
- [73] Trevor Standley, Amir Zamir, Dawn Chen, Leonidas Guibas, Jitendra Malik, and Silvio Savarese. Which tasks should be learned together in multi-task learning? In *International Conference on Machine Learning*, pages 9120–9132. PMLR, 2020. 1
- [74] Baochen Sun and Kate Saenko. Deep coral: Correlation alignment for deep domain adaptation. In *European Conference on Computer Vision*, pages 443–450. Springer, 2016. 2, 7, 3, 4, 5
- [75] Yi Tay, Zhe Zhao, Dara Bahri, Don Metzler, and Da-Cheng Juan. Hypergrid transformers: Towards a single model for multiple tasks. 2021. 2
- [76] Eric Tzeng, Judy Hoffman, Ning Zhang, Kate Saenko, and Trevor Darrell. Deep domain confusion: Maximizing for domain invariance. *arXiv preprint arXiv:1412.3474*, 2014. 2
- [77] Dmitry Ulyanov, Andrea Vedaldi, and Victor Lempitsky. Instance normalization: The missing ingredient for fast stylization. *arXiv preprint arXiv:1607.08022*, 2016. 6
- [78] Laurens Van der Maaten and Geoffrey Hinton. Visualizing data using t-SNE. *Journal of machine learning research*, 9(11), 2008. 6
- [79] Vladimir Vapnik. *The Nature of Statistical Learning Theory*. Springer science & business media, 1999. 7, 8, 3, 4, 5
- [80] Hemanth Venkateswara, Jose Eusebio, Shayok Chakraborty, and Sethuraman Panchanathan. Deep hashing network for unsupervised domain adaptation. In *Proceedings of the IEEE Conference on Computer Vision and Pattern Recognition*, pages 5018–5027, 2017. 5, 2
- [81] Tomer Volk, Eyal Ben-David, Ohad Amosy, Gal Chechik, and Roi Reichart. Example-based hypernetworks for out-of-distribution generalization. *arXiv preprint arXiv:2203.14276*, 2022. 2
- [82] Riccardo Volpi, Hongseok Namkoong, Ozan Sener, John C. Duchi, Vittorio Murino, and Silvio Savarese. Generalizing to unseen domains via adversarial data augmentation. *Advances in neural information processing systems*, 31, 2018. 2
- [83] Johannes Von Oswald, Christian Henning, João Sacramento, and Benjamin F. Grewe. Continual learning with hypernetworks. *arXiv preprint arXiv:1906.00695*, 2019. 2
- [84] Jindong Wang, Wenjie Feng, Yiqiang Chen, Han Yu, Meiyu Huang, and Philip S. Yu. Visual domain adaptation with manifold embedded distribution alignment. In *Proceedings of the 26th ACM International Conference on Multimedia*, pages 402–410, 2018. 2
- [85] Jindong Wang, Cuiling Lan, Chang Liu, Yidong Ouyang, Tao Qin, Wang Lu, Yiqiang Chen, Wenjun Zeng, and Philip

- Yu. Generalizing to unseen domains: A survey on domain generalization. *IEEE Transactions on Knowledge and Data Engineering*, 2022. 1, 3
- [86] Mei Wang and Weihong Deng. Deep visual domain adaptation: A survey. *Neurocomputing*, 312:135–153, 2018. 1, 3
- [87] Shen Yan, Huan Song, Nanxiang Li, Lincan Zou, and Liu Ren. Improve unsupervised domain adaptation with mixup training. *arXiv preprint arXiv:2001.00677*, 2020. 7, 3, 4, 5
- [88] Xiangyu Yue, Yang Zhang, Sicheng Zhao, Alberto Sangiovanni-Vincentelli, Kurt Keutzer, and Boqing Gong. Domain randomization and pyramid consistency: Simulation-to-real generalization without accessing target domain data. In *Proceedings of the IEEE/CVF International Conference on Computer Vision*, pages 2100–2110, 2019. 2
- [89] Seniha Esen Yuksel, Joseph N. Wilson, and Paul D. Gader. Twenty years of mixture of experts. *IEEE transactions on neural networks and learning systems*, 23(8):1177–1193, 2012. 1
- [90] Hongyi Zhang, Moustapha Cisse, Yann N Dauphin, and David Lopez-Paz. Mixup: Beyond empirical risk minimization. *arXiv preprint arXiv:1710.09412*, 2017. 2
- [91] Hanlin Zhang, Yi-Fan Zhang, Weiyang Liu, Adrian Weller, Bernhard Schölkopf, and Eric P Xing. Towards principled disentanglement for domain generalization. In *Proceedings of the IEEE/CVF Conference on Computer Vision and Pattern Recognition*, pages 8024–8034, 2022. 2
- [92] Marvin Zhang, Henrik Marklund, Nikita Dhawan, Abhishek Gupta, Sergey Levine, and Chelsea Finn. Adaptive risk minimization: Learning to adapt to domain shift. *Advances in Neural Information Processing Systems*, 34:23664–23678, 2021. 7, 3, 4, 5
- [93] Dominic Zhao, Johannes von Oswald, Seijin Kobayashi, João Sacramento, and Benjamin F. Grewe. Meta-learning via hypernetworks. 2020. 2
- [94] Tao Zhong, Zhixiang Chi, Li Gu, Yang Wang, Yuanhao Yu, and Jin Tang. Meta-DMoE: Adapting to Domain Shift by Meta-Distillation from Mixture-of-Experts. *arXiv preprint arXiv:2210.03885*, 2022. 1, 3
- [95] Kaiyang Zhou, Ziwei Liu, Yu Qiao, Tao Xiang, and Chen Change Loy. Domain generalization: A survey. *IEEE Transactions on Pattern Analysis and Machine Intelligence*, 2022. 1, 3
- [96] Kaiyang Zhou, Yongxin Yang, Timothy Hospedales, and Tao Xiang. Learning to generate novel domains for domain generalization. In *European Conference on Computer Vision*, pages 561–578. Springer, 2020. 2
- [97] Kaiyang Zhou, Yongxin Yang, Yu Qiao, and Tao Xiang. Domain adaptive ensemble learning. *IEEE Transactions on Image Processing*, 30:8008–8018, 2021. 3
- [98] Kaiyang Zhou, Yongxin Yang, Yu Qiao, and Tao Xiang. Domain generalization with mixstyle. *arXiv preprint arXiv:2104.02008*, 2021. 2
- [99] Barret Zoph, Irwan Bello, Sameer Kumar, Nan Du, Yanping Huang, Jeff Dean, Noam Shazeer, and William Fedus. Designing effective sparse expert models. *arXiv preprint arXiv:2202.08906*, 2022. 2

HMOE: Hypernetwork-based Mixture of Experts for Domain Generalization

Supplementary Material

A. Toy Regression Problem

In the paper, we apply HMOE to the domain generalization problem in the field of image classification. In fact, HMOE is applicable to a wide range of problems beyond DG that are troubled by heterogeneous patterns. In this section, to demonstrate the versatility of HMOE, we apply it to a toy regression problem to learn a one-dimensional piece-wise function (*i.e.*, a discontinuous function) consisting of multiple different functions. This toy regression problem will also provide us with an intuitive understanding of the learning dynamics of HMOE, such as how the gate values evolve and how experts become specialized gradually.

We define a piece-wise function as follows:

$$f(x) = \begin{cases} -x - 2 & \text{if } -3 \leq x < -1 \\ x^2 & \text{if } -1 \leq x \leq 1 \\ \sin(\pi x) & \text{if } 1 < x \leq 3 \end{cases} \quad (11)$$

Using $f(x)$, we generate 10, 20, and 30 data points uniformly in three intervals: $[-3, -1.1]$, $[-1, 1]$ and $[1.1, 3]$, respectively. Unequal data points are used to simulate a naturally unbalanced expert load. And then we fit HMOE to these data points.

HMOE uses three embedding vectors of dimension $D = 8$, which are initialized using the standard normal distribution. All networks of HMOE are MLPs with 32 hidden units. The featurizer is a three-layer MLP whose input size is 1 and output size is 32. The encoder is a three-layer whose input size is 1 and output size is D . The classifier is a two-layer MLP whose input size is 32 and output size is 1. The hypernetwork is a four-layer MLP whose input size is D and output size is the total number of learnable parameters (*i.e.*, weights and biases) of the classifier. In addition, all MLPs use the SiLU activation function [31] except the output layers.

We employ \mathcal{L}_y (use MSE as the loss function), \mathcal{L}_{en} , and \mathcal{L}_{kl} with $\lambda_y = 1$, $\lambda_{en} = 0.5$, and $\lambda_{kl} = 0.1$. HMOE is trained using Adam [38] with learning rate 0.001 over 20,000 epochs. The evolution of the experts' outputs and gates values with respect to training epochs is shown in Fig. 8. We can see that three experts compete with each other and gradually locate their positions, and HMOE manages to identify three intervals even with imbalanced data. We also compare three modes of inference, *i.e.*, MIX, MAX, and OOD, as shown in Fig. 9.

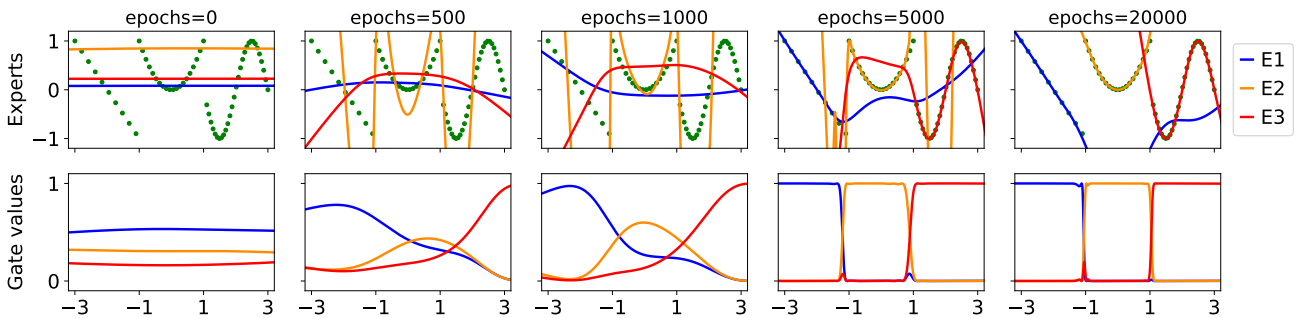


Figure 8: A toy regression problem. We generate some data points using a piece-wise function in three intervals and fit HMOE with three embedding vectors to these points. HMOE well identifies three intervals and experts also become specialized.

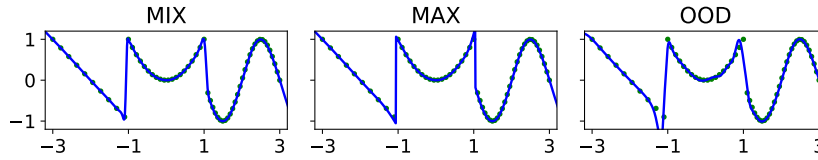


Figure 9: Three modes of inference for the toy regression problem

B. DomainBed

B.1. Description and visualization of datasets

Dataset	Domains						# of classes	# of samples	Image size
ColoredMNIST [2]	+90%	+80%	-90%				2	70,000	(2, 28, 28)
				<i>(degree of correlation between color and label)</i>					
RotatedMNIST [24]	0°	15°	30°	45°	60°	75°	10	70,000	(1, 28, 28)
VLCS [17]	Caltech101	LabelMe	SUN09	VOC2007			5	10,729	(3, 224, 224)
PACS [43]	Art	Cartoon	Photo	Sketch			7	9,991	(3, 224, 224)
OfficeHome [80]	Art	Clipart	Product	Real			65	15,588	(3, 224, 224)
TerraIncognita [4]	L100	L38	L43	L46			10	24,788	(3, 224, 224)
					<i>(camera trap location)</i>				

Table 4: Description and visualization of datasets used in our experiments (Adapted from [26])

B.2. Detailed domain generalization results

We provide the domain generalization results of each test domain for each dataset, and the best results are underlined.

Algorithm		+90%	+80%	-90%	Avg
<i>w/ Domain Labels</i>					
IRM [2]		72.5	73.3	10.2	52.0
GroupDRO [65]		73.1	73.2	10.0	52.1
Mixup [87]		72.7	73.4	10.1	52.1
MLDG [42]		71.5	73.1	9.8	51.5
CORAL [74]		71.6	73.1	9.9	51.5
MMD [45]		71.4	73.1	9.9	51.5
DANN [22]		71.4	73.1	10.0	51.5
CDANN [47]		72.0	73.0	10.2	51.7
MTL [5]		70.9	72.8	10.5	51.4
ARM [92]		82.0	76.5	10.2	56.2
VREx [39]		72.4	72.9	10.2	51.8
HMOE-DL	MIX	71.8	72.9	10.1	51.6
	MAX	71.9	73.1	10.1	51.7
	OOD	71.9	73.2	10.1	51.7
<i>w/o Domain Labels</i>					
ERM [79]		71.7	72.9	10.0	51.5
RSC [32]		71.9	73.1	10.0	51.7
SagNet [57]		71.8	73.0	10.3	51.7
HMOE-DN	MIX	72.0	73.0	10.7	51.9
	MAX	72.0	73.0	10.7	51.9
	OOD	72.0	73.0	10.7	51.9
HMOE-ND	MIX	71.6	73.2	10.1	51.6
	MAX	71.9	73.2	10.2	51.7
	OOD	71.6	73.5	10.1	51.7

Table 5: Domain generalization results on ColoredMNIST

Algorithm		0	15	30	45	60	75	Avg
<i>w/ Domain Labels</i>								
IRM [2]		95.5	98.8	98.7	98.6	98.7	95.9	97.7
GroupDRO [65]		95.6	98.9	98.9	99.0	98.9	96.5	98.0
Mixup [87]		95.8	98.9	98.9	98.9	98.8	96.5	98.0
MLDG [42]		95.8	98.9	99.0	98.9	99.0	95.8	97.9
CORAL [74]		95.8	98.8	98.9	99.0	98.9	96.4	98.0
MMD [45]		95.6	98.9	99.0	99.0	98.9	96.0	97.9
DANN [22]		95.0	98.9	99.0	99.0	98.9	96.3	97.8
CDANN [47]		95.7	98.8	98.9	98.9	98.9	96.1	97.9
MTL [5]		95.6	99.0	99.0	98.9	99.0	95.8	97.9
ARM [92]		96.7	99.1	99.0	99.0	99.1	96.5	98.2
VREx [39]		95.9	99.0	98.9	98.9	98.7	96.2	97.9
HMOE-DL	MIX	94.5	97.7	98.8	98.7	99.0	94.9	97.3
	MAX	94.1	97.9	98.5	98.5	98.6	94.7	97.0
	OOD	95.0	97.9	98.6	98.9	99.1	94.7	97.4
<i>w/o Domain Labels</i>								
ERM [79]		95.9	98.9	98.8	98.9	98.9	96.4	98.0
RSC [32]		94.8	98.7	98.8	98.8	98.9	95.9	97.6
SagNet [57]		95.9	98.9	99.0	99.1	99.0	96.3	98.0
HMOE-DN	MIX	94.1	98.6	98.7	98.6	99.0	95.9	97.5
	MAX	94.0	98.6	98.7	98.6	98.8	95.9	97.4
	OOD	94.0	98.6	98.7	98.6	99.0	95.9	97.5
HMOE-ND	MIX	94.1	98.6	98.7	98.6	99.0	95.9	97.5
	MAX	94.0	98.6	98.7	98.6	98.8	95.9	97.4
	OOD	94.0	98.6	98.7	98.6	99.0	95.9	97.5

Table 6: Domain generalization results on RotatedMNIST

Algorithm		Caltech101	LabelMe	SUN09	VOC2007	Avg
<i>w/ Domain Labels</i>						
IRM [2]		98.6	64.9	73.4	77.3	78.5
GroupDRO [65]		97.3	63.4	69.5	76.7	76.7
Mixup [87]		98.3	64.8	72.1	74.3	77.4
MLDG [42]		97.4	65.2	71.0	75.3	77.2
CORAL [74]		98.3	66.1	73.4	77.5	78.8
MMD [45]		97.7	64.0	72.8	75.3	77.5
DANN [22]		99.0	65.1	73.1	77.2	78.6
CDANN [47]		97.1	65.1	70.7	77.1	77.5
MTL [5]		97.8	64.3	71.5	75.3	77.2
ARM [92]		98.7	63.6	71.3	76.7	77.6
VREx [39]		98.4	64.4	74.1	76.2	78.3
HMOE-DL	MIX	97.7	62.3	72.0	74.8	76.7
	MAX	97.0	63.6	73.2	76.7	77.6
	OOD	97.0	63.4	72.0	74.9	76.8
<i>w/o Domain Labels</i>						
ERM [79]		97.7	64.3	73.4	74.6	77.5
RSC [32]		97.9	62.5	72.3	75.6	77.1
SagNet [57]		97.9	64.5	71.4	77.5	77.8
HMOE-DN	MIX	97.1	63.8	71.2	75.1	76.8
	MAX	97.4	63.4	70.9	74.8	76.6
	OOD	96.4	62.9	69.3	74.7	75.8
HMOE-ND	MIX	95.8	65.7	72.4	72.5	76.6
	MAX	97.3	61.7	72.1	76.1	76.8
	OOD	96.9	61.8	72.0	76.0	76.7

Table 7: Domain generalization results on VLCS

Algorithm		Art	Cartoon	Photo	Sketch	Avg
<i>w/ Domain Labels</i>						
IRM [2]		84.8	76.4	96.7	76.1	83.5
GroupDRO [65]		83.5	79.1	96.7	78.3	84.4
Mixup [87]		86.1	78.9	97.6	75.8	84.6
MLDG [42]		85.5	80.1	97.4	76.6	84.9
CORAL [74]		88.3	80.0	97.5	78.8	86.2
MMD [45]		86.1	79.4	96.6	76.5	84.6
DANN [22]		86.4	77.4	97.3	73.5	83.6
CDANN [47]		84.6	75.5	96.8	73.5	82.6
MTL [5]		87.5	77.1	96.4	77.3	84.6
ARM [92]		86.8	76.8	97.4	79.3	85.1
VREx [39]		86.0	79.1	96.9	77.7	84.9
HMOE-DL	MIX	84.1	77.3	96.3	76.4	83.5
	MAX	82.9	78.6	95.9	78.1	83.9
	OOD	85.0	78.3	95.3	79.4	84.5
<i>w/o Domain Labels</i>						
ERM [79]		84.7	80.8	97.2	79.3	85.5
RSC [32]		85.4	79.7	97.6	78.2	85.2
SagNet [57]		87.4	80.7	97.1	80.0	86.3
HMOE-DN	MIX	83.9	82.3	95.0	77.9	84.8
	MAX	84.7	82.4	96.4	76.9	85.1
	OOD	83.9	80.2	95.6	80.1	84.9
HMOE-ND	MIX	88.8	78.9	96.6	73.9	84.5
	MAX	88.8	82.7	95.7	79.1	86.6
	OOD	88.9	84.3	95.7	79.0	87.0

Table 8: Domain generalization results on PACS

Algorithm		Art	Clipart	Product	Real	Avg
<i>w/ Domain Labels</i>						
IRM [2]		58.9	52.2	72.1	74.0	64.3
GroupDRO [65]		60.4	52.7	75.0	76.0	66.0
Mixup [87]		62.4	54.8	76.9	78.3	68.1
MLDG [42]		61.5	53.2	75.0	77.5	66.8
CORAL [74]		65.3	54.4	76.5	78.4	68.7
MMD [45]		60.4	53.3	74.3	77.4	66.3
DANN [22]		59.9	53.0	73.6	76.9	65.9
CDANN [47]		61.5	50.4	74.4	76.6	65.8
MTL [5]		61.5	52.4	74.9	76.8	66.4
ARM [92]		58.9	51.0	74.1	75.2	64.8
VREx [39]		60.7	53.0	75.3	76.6	66.4
HMOE-DL	MIX	59.5	50.5	73.6	75.2	64.7
	MAX	58.5	47.7	72.5	74.1	63.2
	OOD	58.6	49.9	72.8	73.7	63.7
<i>w/o Domain Labels</i>						
ERM [79]		61.3	52.4	75.8	76.6	66.5
RSC [32]		60.7	51.4	74.8	75.1	65.5
SagNet [57]		63.4	54.8	75.8	78.3	68.1
HMOE-DN	MIX	59.4	52.9	74.6	74.7	65.4
	MAX	60.0	52.1	74.6	74.9	65.4
	OOD	60.2	52.5	73.6	74.7	65.3
HMOE-ND	MIX	60.0	52.4	74.3	75.1	65.5
	MAX	60.0	52.4	73.3	76.3	65.5
	OOD	60.0	54.1	72.8	75.6	65.6

Table 9: Domain generalization results on OfficeHome

Algorithm		L100	L38	L43	L46	Avg
<i>w/ Domain Labels</i>						
IRM [2]		54.6	39.8	56.2	39.6	47.6
GroupDRO [65]		41.2	38.6	56.7	36.4	43.2
Mixup [87]		59.6	42.2	55.9	33.9	47.9
MLDG [42]		54.2	44.3	55.6	36.9	47.7
CORAL [74]		51.6	42.2	57.0	39.8	47.6
MMD [45]		41.9	34.8	57.0	35.2	42.2
DANN [22]		51.1	40.6	57.4	37.7	46.7
CDANN [47]		47.0	41.3	54.9	39.8	45.8
MTL [5]		49.3	39.6	55.6	37.8	45.6
ARM [92]		49.3	38.3	55.8	38.7	45.5
VREx [39]		48.2	41.7	56.8	38.7	46.4
HMOE-DL	MIX	43.1	44.9	55.8	36.1	45.0
	MAX	42.2	38.1	55.0	37.4	43.2
	OOD	43.0	42.2	54.6	36.3	44.0
<i>w/o Domain Labels</i>						
ERM [79]		49.8	42.1	56.9	35.7	46.1
RSC [32]		50.2	39.2	56.3	40.8	46.6
SagNet [57]		53.0	43.0	57.9	40.4	48.6
HMOE-DN	MIX	54.0	43.6	58.3	38.8	48.7
	MAX	54.0	47.0	58.3	38.8	49.5
	OOD	54.1	42.1	58.3	39.0	48.4
HMOE-ND	MIX	58.8	41.8	56.1	36.8	48.4
	MAX	44.7	41.8	56.5	36.8	45.0
	OOD	53.4	41.8	55.6	37.5	47.1

Table 10: Domain generalization results on TerraIncognita